ChemComm

COMMUNICATION

View Article Online
View Journal | View Issue

Photocatalytic reforming of glucose under visible light over morphology controlled Cu_2O: efficient charge separation by crystal facet engineering†

Cite this: *Chem. Commun.*, 2014, 50, 192

Received 22nd August 2013,
Accepted 25th October 2013

DOI: 10.1039/c3cc46423g

www.rsc.org/chemcomm

Longzhou Zhang, Jinwen Shi, Maochang Liu, Dengwei Jing* and Liejin Guo

Multifaceted Cu_2O with controlled crystal facet exposure was synthesized *via* a facile one-step method. It was found that photo-generated electrons prefer to accumulate on high index planes, while holes tend to migrate to {100} facets of a Cu_2O polyhedron, leading to efficient charge separation and enhanced photocatalytic reforming of glucose.

Photocatalytic hydrogen production under solar light has been considered as one of the most promising routes for renewable energy production.[1,2] Traditionally, methanol, Na_2S, Na_2SO_3, EDTA, *etc.* are often used in the photocatalytic reactions as electron donors for hydrogen production.[3] On the other hand, biomass is one of the most versatile renewable resources. If glucose, as a model compound of biomass, could be employed as an electron donor, the process can be considered completely renewable.

The feasibility of photocatalytic hydrogen production from glucose has been demonstrated as early as 1980 by Kawai *et al.*[4,5] However, most of the studies are conducted under UV light, owing to either the wide band gap or lower conduction band positions of the employed oxide semiconductors.[6,7]

Cuprous oxide, Cu_2O, is an attractive p-type oxide semiconductor with a direct bandgap of 2 eV and a theoretical light-to-hydrogen conversion efficiency of 18%.[8] Theoretically, due to its cubic feature, Cu_2O can grow into multi shapes, such as cubic and octahedral morphology.[9] However, these multi-faceted Cu_2O were often synthesized by a two-step approach. For instance, face concaved Cu_2O with multi facets was often synthesized from cubic seeds.[10] From the viewpoint of practical photocatalytic applications, Cu_2O prepared by complicated multi-step approaches is apparently not favoured.

In this communication, Cu_2O was synthesized by a facile one-step method with carefully controlled reaction time. In a typical process of synthesis, 0.12 g $Cu(NO_3)_2$ and 0.3 g tartaric acid were dissolved in 40 mL deionized water, and stirred for 5 min. Then 0.22 g NaOH was added to the aqueous solution, the colour of the solution changed to dark blue instantly. 0.09 g glucose was then added to the system. The beaker was placed into an oven, and kept at 105 °C for a fixed time. The resulting erythrine precipitate was centrifuged and washed with ethyl alcohol and deionized water, respectively, and dried under vacuum at 60 °C for 5 hours.

For photocatalytic hydrogen evolution, 0.1 g photocatalyst powder was dispersed using a magnetic stirrer in a side irradiated photocatalytic reactor containing aqueous solution of glucose (0.0125 mol L^{-1}) and NaOH (0.1 mol L^{-1}). The reaction cell was connected to a gas circulation system and the hydrogen evolved was analyzed using an on-line TCD gas chromatograph (NaX zeolite column, argon as a carrier gas). The photocatalysts were irradiated with visible light from a 300 W Xe lamp and the UV part of the light was removed using a cut-off filter (λ > 420 nm). The gas product was automatically sampled and analyzed by GC every 10 minutes during photocatalytic reaction. Before the photocatalytic reaction, the reactor was alternatively evacuated using a vacuum pump and flushed by argon several times to ensure complete removal of oxygen.

SEM images of Cu_2O prepared at different reaction times are shown in Fig. S1 (ESI†). The UV-vis absorption patterns and XRD results are given in Fig. S2 and S3 (ESI†), respectively. For easy observation of the morphological evolution of Cu_2O, representative SEM images of a single Cu_2O polyhedron prepared at different stages were taken. As shown in Fig. 1, cubic Cu_2O with 6 exposed {100} facets was obtained after 30 min of reaction. Interestingly, the cubic shape changed into a cubooctahedron after 60 min of reaction. The eight corners of particles were etched and some {111} facets evolved. The polyhedron now has both {100} and {111} exposed facets. After 90 min of reaction, as shown in Fig. 1c, {111} facets were further split into 3 new facets. These 3 high index facets together with {111} facets formed a pyramid, the apex angle is calculated to be 119.8°, and the included angle between these 3 high index facets and {111} facets is 6.3°. According to Steno's law, for crystals of different shape and size,

International Research Center for Renewable Energy, State Key Laboratory of Multiphase Flow in Power Engineering, Xi'an Jiaotong University, Xi'an 710049, China. E-mail: dwjing@mail.xjtu.edu.cn

† Electronic supplementary information (ESI) available. See DOI: 10.1039/c3cc46423g

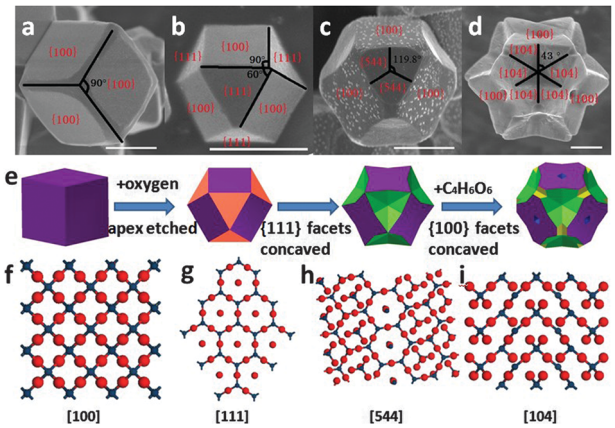

Fig. 1 Morphological evolution of Cu_2O prepared at different reaction times, (a) 30 min, (b) 60 min, (c) 90 min and (d) 120 min. All scale bars are 1 μm. Schematic illustration for the formation of Cu_2O (e). Different crystal facets, (f) [100], (g) [111], (h) [544] and (i) [104].

the included angle between planes is a constant. The exposed high index plane can thus be well defined. According to the equation of included angle for a cubic system (eqn (1)), the new facets were confirmed to be [544]. Fig. 1d shows the crystal morphology of Cu_2O after 120 min of reaction. The {544} facets continue to be etched and split into even smaller planes. Similarly, the plane can be defined as {104} facets. Meanwhile, the {100} facets were also observed to experience an evident change. The surface of {100} facets was gradually concaved, and a nano sized hole could be observed in the center of {100} facets. Based on the above observation, the morphological evolution process of the Cu_2O was schematically illustrated (Fig. 1e).

$$\theta = \cos^{-1}\left\{\frac{h_1h_2 + k_1k_2 + l_1l_2}{\sqrt{h_1^2 + k_1^2 + l_1^2}\sqrt{h_2^2 + k_2^2 + l_2^2}}\right\} \quad (1)$$

Basically, the growth of a crystal should follow a facet selective principle. In our case, oxygen dissolved in the solution is supposed to play a very important role in the facet exposure control. This is further demonstrated by our control experiment carried out in the absence of oxygen during morphological evolution of Cu_2O. As shown in Fig. S4 (ESI†) negligible etching could be observed when oxygen was evacuated from the reaction system. Slight etching occurring on the corners of some nanocubes could be attributed to the residual trace oxygen that cannot be completely removed by evacuation. A similar oxidative etching mechanism has been reported for the synthesis of Ag nanocubes.[11] It was found that oxygen dissolved in the solution oxidizes some surface atoms of Ag nanocubes and eventually generates truncated cubes. Accordingly, the oxidative etching of Cu_2O is described as eqn (2).

$$2Cu_2O + O_2 + 4H_2O \rightarrow 4Cu^{2+} + 8OH^- \quad (2)$$

It is assumed that atoms located on the edges and corners are unsaturated and should have higher surface energy, so they are more easily etched. The formation of multifaceted Cu_2O must be a result of competition between preferential growth and selective oxidative etching. In our case, Cu_2O kept growing to relatively larger size with its surface being selectively etched at the same time. Competition between crystal growth and new facet generation, therefore higher surface area, is expected. In fact, BET analysis showed the surface areas of 2.7, 3.7, 2.0 and 7.6 $m^2\ g^{-1}$, respectively, for Cu_2O prepared at 30 min, 60 min, 90 min and 120 min. At the same time, as shown by size distribution analysis in Fig. S1 (see Fig. S5, ESI†), the Cu_2O particle indeed underwent a slow size growth, with its size distribution becoming more homogeneous.

Due to the difference in electro-negativities between Cu and O atoms, the {100} facets of Cu_2O crystals are predominated by only Cu or O atoms, leading to the electrically neutral state of {100} facets. However, the {111} facets are formed by both Cu and O atoms and surface Cu atoms with dangling bonds on {111} facets can be positively charged and therefore strongly protected by a negatively charged capping agent.[12] Accordingly, under our synthesis conditions, negatively charged tartaric acid should prefer to be absorbed on {111} facets forming a protecting layer and avoiding or, at least, retarding oxidative etching of these facets at certain part. As for the pits in the center of {100} facets and the concave {100} facets, the incompact absorption of tartaric acid on {100} facets is believed to be one important factor. Nevertheless, a clear understanding of the role of tartaric acid apparently needs more detailed work. Notably, Sun *et al.* reported that ethanol molecules can lead to the formation of pits on {111} facets of Cu_2O, which could be informative to our future study.[13]

Fig. 2 shows the result of 6 hours of hydrogen production over the as-prepared Cu_2O with various morphologies. The photocatalytic activity of cubic Cu_2O is the lowest, while the Cu_2O concaved with apex and {100} facets, which also has the largest surface area of 7.6 $m^2\ g^{-1}$, displayed the highest activity. Apparently, Cu_2O with more high-index planes showed higher activity toward photocatalytic reforming of glucose under visible light. The resultant photocatalytic activity should be closely related to the topography of Cu_2O. Here we suppose that there must be preferential distribution of electrons and holes on

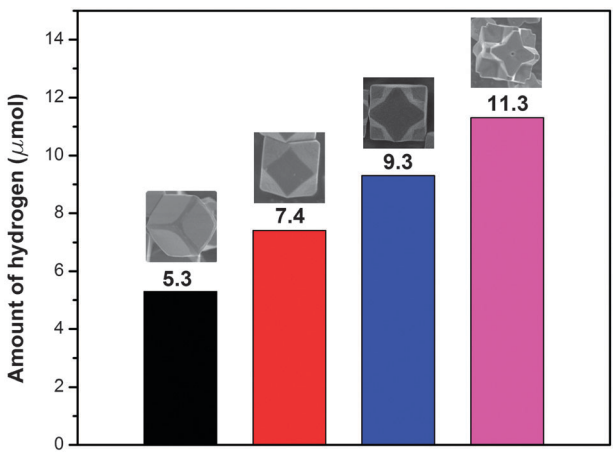

Fig. 2 The performance of photocatalytic hydrogen production under visible light irradiation over Cu_2O with different morphologies.

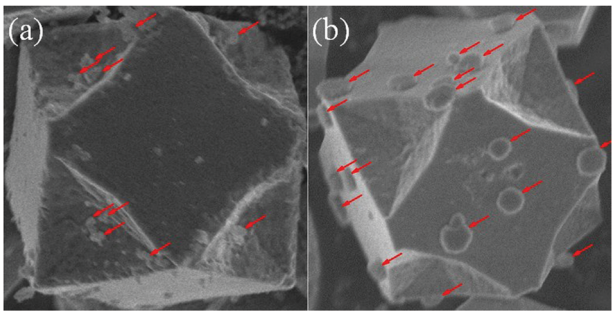

Fig. 3 SEM images of Cu_2O loaded with Pt (a) and PbO_2 (b), respectively.

{100} facets and those high index planes as well. To verify this assumption, Pt and PbO_2 were photo-deposited on Cu_2O shown in Fig. 1d by photo-reduction and photo-oxidation, respectively. As indicated by black arrows in Fig. 3, PbO_2 was loaded only on {100} facets and Pt was loaded mainly on the apices with a high index. As reported, the photo-deposited Pt and PbO_2 could be the indicators of photogenerated electrons and holes, respectively.[14] Our results showed that the photogenerated electrons and holes can be separated among the different facets of Cu_2O semiconductor crystals. The accumulation of electrons on the high index facets and holes on {100} facets only corresponds well to the function of reduction and oxidation facets, respectively. It is reasonable to deduce that the accumulation of electrons and holes originates from charge separation on different facets. The origin of the charge separation on different crystal facets of TiO_2 has been already estimated by theoretical calculation.[15] A slight energy difference in the valence and conduction bands between two different facets could drive electron transfer from one facet to another, leading to the accumulation of electrons and holes separately on the corresponding facets. Accordingly, the successful charge separation is supposed to be responsible for the significantly enhanced photocatalytic activity.

Moreover, it is also known that the reduction of H^+ by photogenerated electrons is the rate-limiting step for photocatalytic hydrogen production.[3] Considering the preferential accumulation of electrons on the high-index facets of Cu_2O, it is therefore reasonable that Cu_2O with more high-index facets showed higher photocatalytic activity toward photocatalytic reforming of glucose.

The authors gratefully acknowledge the financial support from the National Natural Science Foundation of China (No. 21276206, 51302212), the Fundamental Research Funds for the Central Universities (No. xjj2012117, 2013JDHZ20) and the China Postdoctoral Science Foundation (No. 2013M540745).

Notes and references

1 X. Chen, S. Shen, L. Guo and S. Mao, *Chem. Rev.*, 2010, **110**, 6503–6570.
2 K. Maeda, K. Teramura, D. Lu and K. Domen, *Nature*, 2006, **440**, 295.
3 A. Kudo and Y. Miseki, *Chem. Soc. Rev.*, 2009, **38**, 253.
4 T. Kawai and T. Sakata, *Nature*, 1980, **286**, 474.
5 M. Kawai, T. Kawai and K. Tamaru, *Chem. Lett.*, 1981, 1185.
6 X. Fu, J. Long and X. Wang, *Int. J. Hydrogen Energy*, 2008, **33**, 6484.
7 Y. Tachibana, L. Vayssieres and J. Durrant, *Nat. Photonics*, 2012, **6**, 511–518.
8 A. Paracchino, V. Laporte, K. Sivula, M. Grätzel and E. Thimsen, *Nat. Mater.*, 2011, **10**, 456–461.
9 J. Teo, Y. Chang and H. Zeng, *Langmuir*, 2006, **22**, 7369.
10 J. Ho and M. Huang, *J. Phys. Chem. C*, 2009, **113**(32), 14159–14164.
11 Y. Xiong, *Chem. Commun.*, 2011, **47**, 1580–1582.
12 J. Y. Ho and M. H. Huang, *J. Phys. Chem. C*, 2009, **113**, 14159–14164.
13 S. Sun, H. You, C. Kong, X. Song, B. Ding and Z. Yang, *CrystEngComm*, 2011, **13**, 2837.
14 R. Li, F. Zhang, D. Wang, J. Yang, M. Li, J. Zhu, X. Zhou, H. Han and C. Li, *Nat. Commun.*, 2013, **4**, 1432.
15 J. Pan, G. Liu, G. Lu and H. Cheng, *Angew. Chem., Int. Ed.*, 2011, **50**, 2133–2137.

